Flux Guides for Permanent-Magnet Machines

John S. Hsu
Senior Member
Oak Ridge National Laboratory*
Post Office Box 2009, MS 8038
Oak Ridge, Tennessee 37831

Key words: *effective flux enhancements, permanent-magnet machines, flux guides, motors, generators, electric vehicle, drives.*

Abstract

A new concept for the enhancement of effective flux of PM machines using flux guides is introduced. An intrinsic demagnetization curve that considers the leakage flux is derived. On the basis of a higher effective flux the stator winding can be more compact; consequently, a lighter stator and a higher efficiency permanent magnet (PM) machine can be obtained. This technology can be used for both PM motors and generators. On the basis of tests conducted on various magnetic path arrangements the "transverse flux machine" is also discussed.

I. INTRODUCTION

PM electric machines are known for having a high power density. The costs of PMs of different materials vary greatly. Research options are using a lower grade PM for cost reduction or increasing power density with a high grade PM. This paper introduces a third option, which is the effective flux enhancement of permanent-magnet machines through the third dimensional flux guides.

The search for a higher power density PM motor is not new. For instance, the well-known European "transverse flux motor" [1] technology is shown in Fig. 1. On the basis of tests conducted on various flux path arrangements, this paper will later discuss theoretical and experimental limitation of the transverse-flux motor.

The pros and cons of various flux path arrangements are studied in this paper. Flux guides are feasible for effective flux enhancements of PM machines. This paper introduces two types of flux guides, which are the stationary type mounted on the stator teeth and the rotating type mounted on the rotor PM poles.

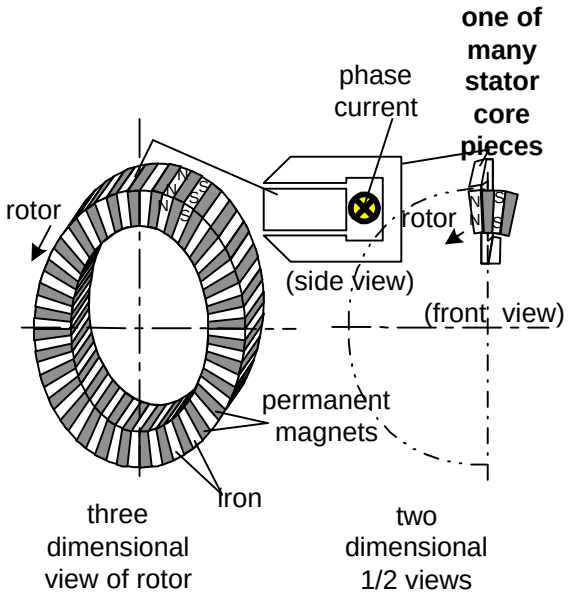

Fig. 1 Geometry of one phase of a transverse flux machine

The stationary flux guides see alternating fluxes. Recent technology development in the pressed powder metallurgy [2] for alternating current (AC) cores enables the practical production of flux guides that have sufficiently high mechanical strength with relatively low AC core losses. The flux in the pressed flux guides can flow in three dimensions without the restrictions imposed on laminations.

The study of the PM requirements for electric propulsion motors and the raw material availability and costs given in [3] are relatively old. Nevertheless, this

*

reference gives a useful picture for tracking the development trend of PM motors for electric vehicles. It might help to understand the need for flux guides to lower the cost and improve the performance of PM machines.

II. THE FIRST LAW (AMPERE'S LAW) OF ELECTROMAGNETIC THEORY

Electromagnetic theory is based on two fundamental laws called the 'circuit laws' [4-6]. The first law (Ampere's law) is: 'The line integral of the magnetic field strength or intensity taken around any closed path is proportional to the total current flowing across any area bounded by that path. In symbols, the first law is

$$\oint H\, dl = \sum I \quad . \tag{1}$$

2.1 Magnetic Field Strength Inside PM Without Current:

Unlike the magnetic flux in a soft magnetic material path, the PM sees flux even when the total current, *SI*, flowing across any area bounded by that path is zero. The total magnetic field strengths inside and outside the PM are equal in magnitude but in opposite directions.

$$H_g \cdot L_g = -H_m \cdot L_m \quad , \tag{2}$$

where the symbol *H* is for the magnetic field strength, *L* is for the length. The suffix *g* is for the air gap, and *m* is for the PM.

2.2 Intrinsic Demagnetization Curve with Leakage Factor:

An intrinsic demagnetization curve that includes the consideration of leakage flux is derived for the evaluation of the PM flux density, *Bm*, and the air-gap flux density, *Bg*. The derivation of the intrinsic demagnetization curve with leakage factor follows.

Fig. 2 shows a simple magnetic path in a uniform thickness. *Ag* represents the air gap area perpendicular to the flux, and the PM area perpendicular to the flux is represented by *Am*. From (1) we have

$$H_g \cdot L_g + H_m \cdot L_m = \sum I \,. \tag{3}$$

For simplification let us assume that the flux is confined in the path shown in Fig. 2; the iron is not saturated with its magnetic field strength close to zero. Magnetic flux must be continuous. Because of the leakage flux the PM flux *BmAm* is greater than the air-gap flux *BgAg* by a leakage factor, s , that is always greater than or equal to 1.

$$s \cdot B_g \cdot A_g = B_m \cdot A_m \,,$$

or

$$B_g = \frac{1}{s} \cdot \frac{A_m}{A_g} \cdot B_m \quad . \tag{4}$$

Substituting (4) into (3) and using the air-gap permeability, m_o , to relate *Bg* to *Hg* give

$$\frac{A_m}{m_0 \cdot A_g \cdot s} \cdot B_m \cdot L_g + H_m \cdot L_m = \sum I \quad .$$

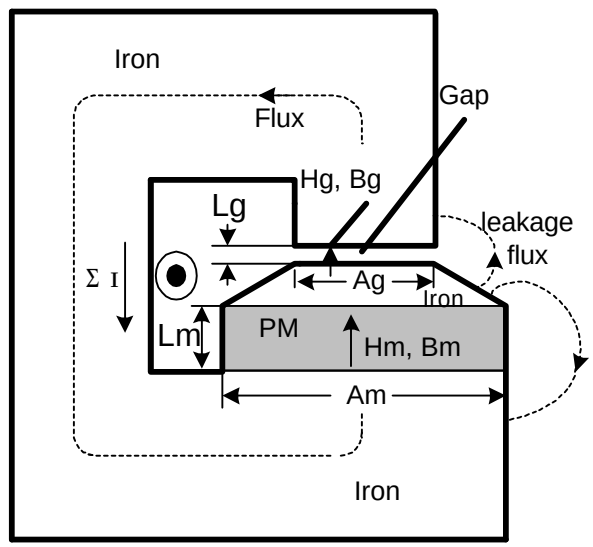

Fig. 2 Flux path with air gap area, *Ag*, PM area, *Am*, and leakage flux.

Simplification gives:

$$B_m - m_0 \cdot s \cdot H_m = -\left[\left(\frac{L_m}{\frac{A_m}{A_g} L_g} + 1\right) m_0 \cdot s\right] \cdot \left(H_m - \frac{\sum I}{\frac{A_m}{A_g} L_g + L_m}\right) \quad . \tag{5}$$

Eqn. (5) represents the intrinsic demagnetization curve that considers the influence of leakage flux by including the leakage factor, σ. This curve is shown in Fig. 3.

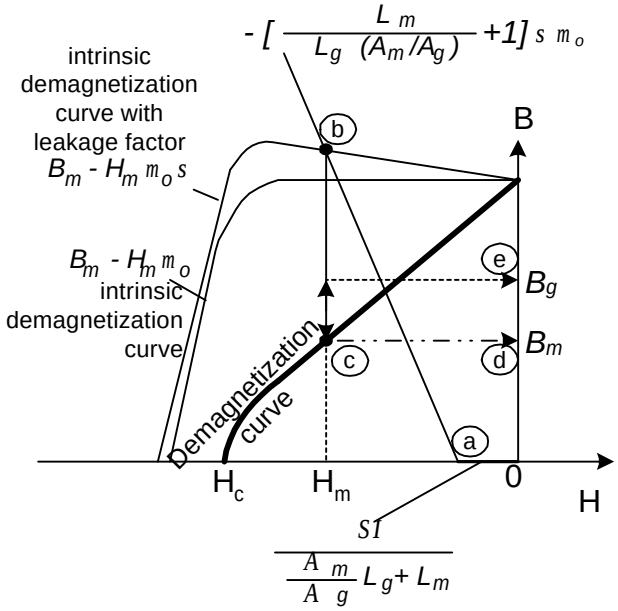

Fig. 3 Obtaining B_m and B_g.

2.3 Flux Densities Evaluation:

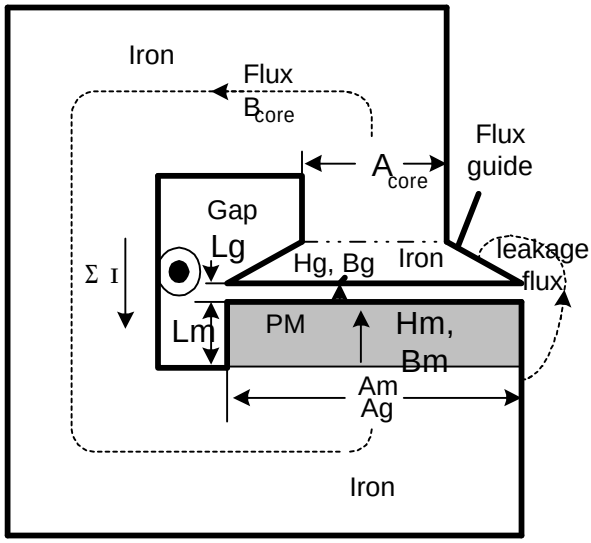

Fig. 5 Flux path with air-gap area, *Ag*, equal to PM area, *Am*.

Fig. 6 shows the finite element flux plots. Fig. 6(a) corresponds to the magnetic path arrangement of Fig. 2 where the air-gap area is less than the PM area. Significant leakage fluxes are shown in the plot. This is also equivalent to the magnetic paths of Fig. 1. Fig. 6(b) shows that the effective flux for the motor is increased when the air-gap area is not less than the magnet area. The flux lines become more dense in the iron core.

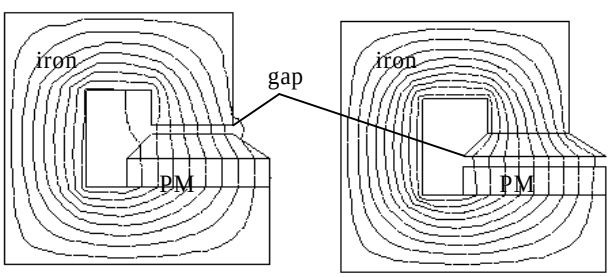

(a) (b)

Fig. 6 Finite element flux plots.

IV. MAGNETIC-PATH PROTOTYPES AND TESTS

4.1 Magnetic-Path Prototypes:

Fig. 7 shows four experimental setups of the magnetic-path arrangements. The air-gap areas of Figs. 7a and 7b defined by the area of the iron piece at the gap are the same but the leakage situations are different. The air-gap areas shown in Figs. 7c and 7d are in their opposite extremes. Fig. 7c has a gap area less than the PM area. It represents the magnetic path shown in Fig. 2. Fig. 7d has a gap area identical to the PM area. The magnetic path of Fig. 7d is shown in Fig. 5. The air gap flux densities are measured through a Bell Model 620 Gaussmeter. The measured results are given in Table 1.

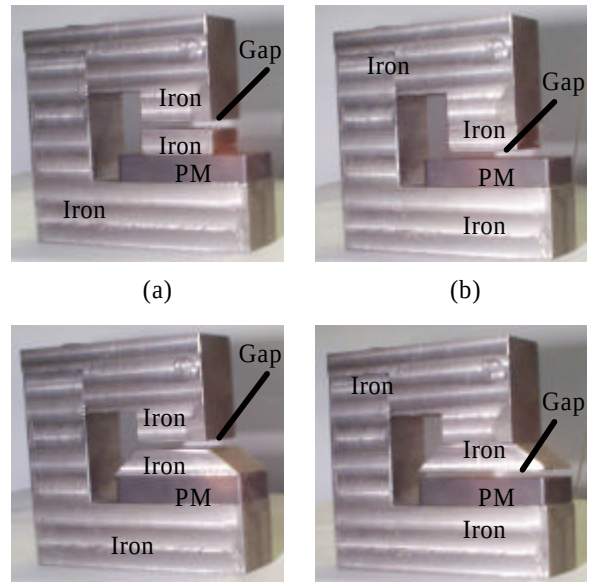

(a) (b)

(c) (d)

Fig. 7 Four experimental setups.

4.2 Test Results:

If the leakage flux were negligible, the air-gap areas of Figs. 7a and 7b, defined by the area of the iron piece at the gap, are the same and the air-gap flux densities between columns (a) and (b) of Table 1 would be the same. However, because of the leakage flux the measured air-gap flux densities between columns (a) and (b) for all three PM and air-gap types are quite different. The lower values of *Bg* in column (a) indicate that the flux path arrangement of Fig. 7a has a stronger leakage flux.

		(a)	(b)	(c)	(d)
Bg	Ceramic #5 0.105” gap 0.387” PM	2.5 kgauss	2.8 kgauss	2.5 kgauss	2.8 kgauss
	Nd+B 0.098” gap 0.394” PM	4.0 kgauss	4.7 kgauss	5.7 kgauss	4.6 kgauss
	Nd+B 0.295” gap 0.197” PM	1.6 kgauss	2.1 kgauss	1.9 kgauss	2.1 kgauss

Table 1 Measured air-gap flux densities of four experimental setups with different air gaps and PM thicknesses.

Test results shown in column (c) and line 2 indicate that the air-gap flux amplification only takes place when the PM grade is high and the air gap is small. The 5.7 kgauss is higher than 4.6 kgauss. The air-gap flux-density amplification disappears when the magnet grade is low (see line 1 of columns (c) and (d)) or the gap is large (see line 3 of columns (c) and (d)).

On the basis of the conclusions observed from the above test results, the air-gap flux density of a transverse-flux machine is very much determined by its leakage flux and air gap. The air-gap flux density of a transverse-flux machine might not be much higher than a conventional PM machine if the leakage flux is high and the air gap is large. However, the author has not found a report showing the tests conducted on a transverse-flux motor for verification.

V. POSSIBLE FLUX GUIDES FOR EFFECTIVE FLUX ENHANCEMENTS OF PM MACHINES

On the basis of the above analyses and tests, two types of flux guide can be used. One is a stationary type of flux guide that is particularly suitable for low grade PMs and/or large air gaps with a flux path arrangement similar to Fig. 5. The other one is a rotating type of flux guide that is particularly suitable for high-grade PMs and with small air gaps.

5.1 Axial-Gap PM Machines with Stationary Flux Guides:

Fig. 8 shows a possible arrangement of an axial-gap PM machine with stationary flux guides extended in the radial directions. The outer and inner edges of the flux guides can be tapered. The flux is collected and directed to the armature teeth of the stator.

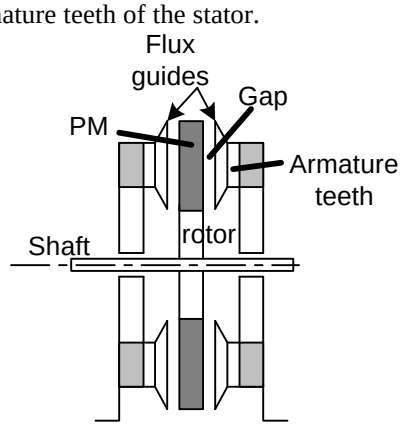

Fig. 8 A possible arrangement of an axial-gap PM machine with stationary flux guides extended in the radial directions.

5.2 Radial-gap PM Machines with Stationary Flux Guides:

Fig. 9 shows a possible arrangement of a radial-gap PM machine with stationary flux guides extended in the axial directions. Again, the large air-gap area enables the flux to flow easily. The flux is collected by the flux guides and directed to the more compacted stator teeth and core.

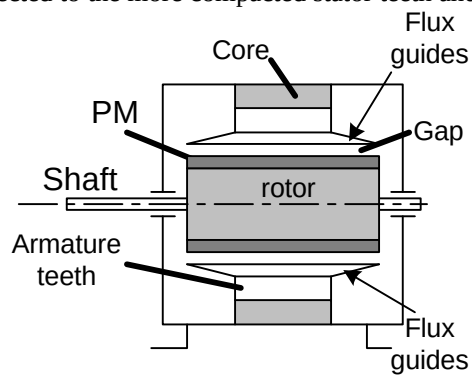

Fig. 9 A possible arrangement of a radial-gap PM machine with stationary flux guides extended in the axial directions.

5.3 Design Considerations of Stationary Flux Guides:

As an example, Fig. 10 shows a possible flux guide of an axial-gap PM machine. The leakage path in the guide is reduced by adding non-magnetic space between the portions that contact the armature teeth. The non-magnetic space can be of air or of a non-magnetic material that can be pressed and joined together with the powder to form a solid component of flux guide.

The flux guides should be low cost, mechanically and thermally sound, with low AC loss, small incremental volume and lightweight. Further, they should add minimal slot leakage to the winding, and be easily and securely attached to the armature teeth. Many of these design goals can be met by the pressed powder metallurgy.

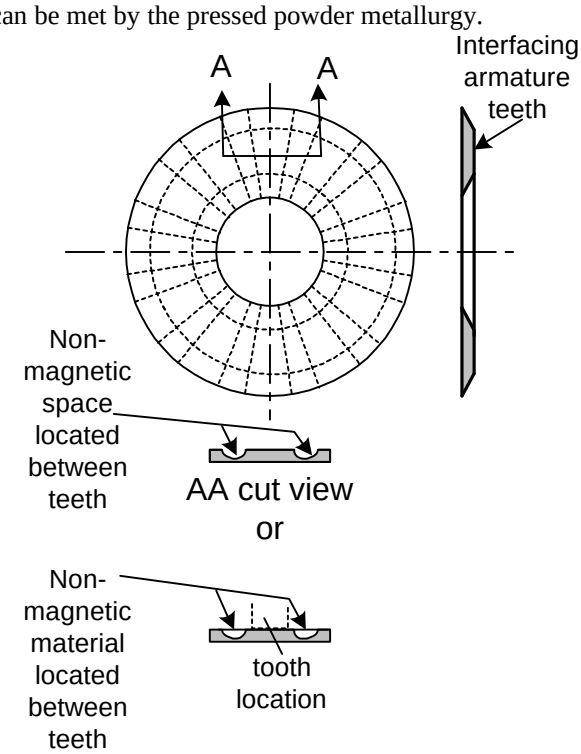

Fig. 10 Possible stationary flux guides of an axial-gap

5.4 Axial-Gap PM Machines with Rotating Flux Guides:

Fig. 11 shows a conceptual cross-sectional view of a multiple-disk axial-gap PM machine with rotating flux guides. The flux guide is mounted on the surface of the PM pole. It is not necessary to used compressed powder for the guide material, because the guide is rotating with the main PM flux. It should be pointed out again that this type of flux guide is only good for high-grade PM materials and with a small air gap.

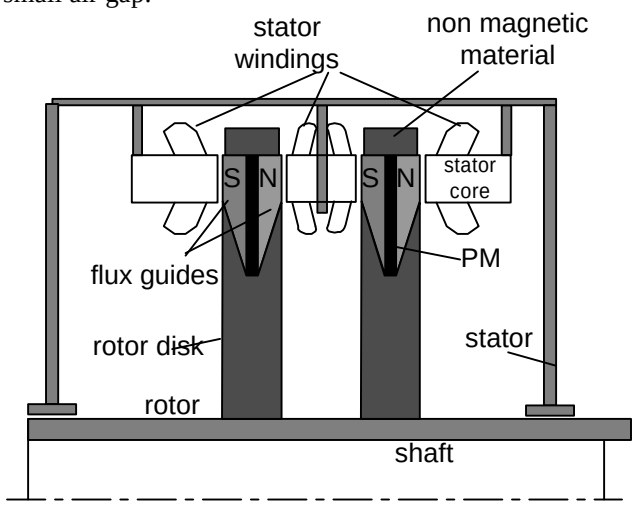

Fig. 11 A rotating flux guide of a multiple-disk axial-gap PM machine.

5.5 Radial-Gap PM Machines with Rotating flux Guides:

Fig. 12 shows the side cross sectional and front views of a radial-gap PM machine with rotating flux guides. This type of flux guide is also only good for high-grade PM materials with a small air gap.

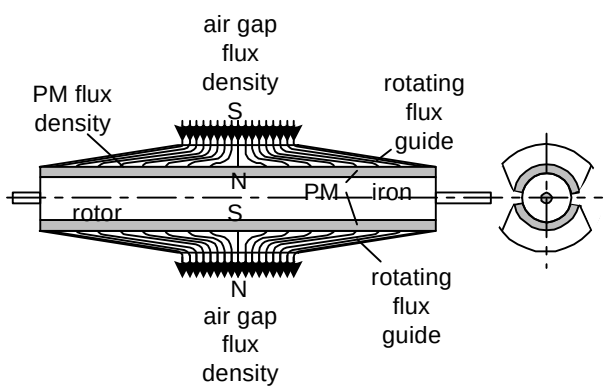

Fig. 12 Radial-gap PM machine with rotating flux guides.

VI. CONCLUSIONS

- A new concept for the enhancement of effective flux of PM machines by using flux guides is introduced.
- Stationary and rotating flux guides are introduced.
- The stationary flux guides are suitable for low-grade PMs and/or large air gaps. The rotating flux guides are suitable for high-grade PMs with small air gaps.
- An intrinsic demagnetization curve with leakage factor is derived for the evaluation of flux densities.
- On the basis of a higher effective flux produced by the flux guides, the stator winding size can be reduced to produce a lighter stator and a higher efficiency PM machine.
- A significant leakage flux may negate the higher power density predicted by an air-gap flux density amplification in a conventional flux focused machine.
- transverse flux machine with an air-gap area less than its PM area and with a significant leakage flux might not have a higher power density than a conventional PM machine.
- Examples of flux-guide structures are given.
- This technology can be used for both PM motors and generators.
- This technology is particularly useful for, but not limited to electric vehicle motor drives and PM generators.

VII ACKNOWLEDGMENT

The author appreciated the support funded by the Office of Advanced Automotive Technologies, U.S. Department of Energy. Encouragement from the Power Electronics and Electric Machine Research Center headed by Mr. Donald Adams, the helpful discussion from Dr. John McKeever, and the building of experimental setups by Mr. S. Michael Jenkins are gratefully acknowledged.

VIII. REFERENCES

[1] A. Mitcham, M. Bolton, “The Transverse Flux Motor: A New Approach to Naval Propulsion,” Proceedings, Naval Symposium on Electric Machines, p.p. 18, July 2831, 1997, The Hotel Viking, Newport, RI.

[2] R. F. Krause, J. H. Bularzik, H. R. Kokal, “High Density Metal Component Manufactured by Powder Metallurgy,” United States Patent No. 5,594,186, January 14, 1997.

[3] Karl Strnat, Study and Review of Permanent Magnets for Electric Vehicle Propulsion Motors, NASA CR-168178 (DOE/NASA/0189-83/2), Prepared for NASA Lewis Research Center under contract DEN 3-189, and for U.S. Department of Energy, Conservation and Renewable Energy, Office of Vehicle and Engine R&D, September, 1983.

[4] Donald G. Fink, John M. Carroll, Standard Handbook for Electrical Engineers, Tenth Edition, McGraw-Hill Book Company, 1969.

[5] Lester R. Moskowitz, Permanent Magnet Design and Application Handbook, 1976, Cahners Books International, Inc., Boston, Massachusetts 02116.

[6] Raymond L. Sanford, Permanent Magnets, Circular of the National Bureau of Standards C448, Issued August 10, 1944, United States Government Printing Office, Washington.

John S. Hsu (Htsui) received a B.S. degree from Tsing-Hua University, Beijing, China, and a Ph.D. degree from Bristol University, England.

He worked in research and development areas for Newman Industry of England, Emerson Electric Company, and later for Westinghouse Electric Corporation. He served as head of the Rotating Machines and Power Electronics Program, Center for Energy Studies, the University of Texas at Austin for four years.

Presently, he is a senior staff scientist of the Power Electronics and Electric Machine Research Center, Oak Ridge National Laboratory. Dr. Hsu is the author or co-author of over one hundred technical papers and reports.